FIN DESIGN FOR FIN-AND-TUBE HEAT EXCHANGER WITH MICROGROOVE SMALL DIAMETER TUBES FOR AIR CONDITIONER

Yifeng Gao[(a)], Ji Song[(a)], Jingdan Gao[(b)], Guoliang Ding[(b)*]

[(a)] International Copper Association Shanghai Office
Shanghai 200020, China, frank.gao@copperalliance.asia
[(b)] Institute of Refrigeration and Cryogenics, Shanghai Jiao Tong University
Shanghai 200240, China, glding@sjtu.edu.cn

ABSTRACT

Optimal louver fins suitable for 5 mm diameter tubes are designed by Computational Fluid Dynamic-based method in this study. Based on the design result, a set of fin-and-tube heat exchangers with 5 mm diameter tubes are tested to develop correlations to predict the performance of new fin-and-tube heat exchanger. According to the experimental results, it is found that water bridge occurs at the bottom of fin with hydrophilic coating, which did not occur in fin-and-tube heat exchangers with 7 mm or 10.33 mm diameter tubes in previous studies. Based on the data, correlation of *j* is developed to predict the heat transfer rate of fin-and-tube heat exchanger with 5 mm diameter tubes. The mean deviations of the proposed *j* correlation are 6.5%.

1. INTRODUCTION

Fin-and-tube heat exchangers are widely used in air conditioners. For lower material cost, fin-and-tube heat exchangers with microgroove small tubes (diameter is smaller than or equal to 5 mm) gradually replace those with 7 mm or larger diameter tubes. When tube diameter decreases from 7 mm to 5 mm, the tube cross-sectional area can be reduced by 49%, and the refrigerant charge can be decreased accordingly. Due to the lower refrigerant charge, greenhouse effect caused by application of high GWP refrigerants may be reduced, and the explosion risk of air conditioners using flammable refrigerants (e.g. R290) can be also obviously decreased. Moreover, with the decrease of tube diameter, the heat exchanger can be more compact if a constant heat exchanger capacity is required; or the heat exchange capacity can be enhanced if a constant heat exchanger size is required.

However, the present fin configuration with large diameter tubes cannot be directly used for smaller tubes due to different configurations of heat exchangers. In fin-and-tube heat exchanger, the permitted fin pitch depends on the tube diameter, and the fin size is related to the balance of fin side heat transfer resistance and tube side heat transfer resistance, so fin configuration with smaller diameter tube is different from that with larger diameter tubes. The mismatching of fin configuration with tubes may decrease heat transfer rate and increase air-side pressure drop. Thus, it is necessary to design a set of suitable fin configurations with smaller diameter tubes.

For fin configuration design, empirical equations developed on the experimental data of heat exchangers are employed due to short time consumption and less resource requirement. However, large deviations will occur between predicted values and experimental data, when the empirical equations (Wang et al., 2002; Ma et al., 2007; Ma et al., 2009) for 7mm or larger diameter tubes are used for predicting performance of heat exchanger with microgroove small tubes. Until now, there are no empirical equations for heat exchanger with microgroove small tubes in literature. Therefore, empirical equations of heat exchanger with microgroove tubes should be developed.

In this study, a set of fins with high heat exchange rate and low air-side pressure drop for 5 mm diameter tubes was designed by computational fluid based method. Based on the design results, heat transfer rate of fin-and-tube heat exchanger with 5 mm diameter tubes were tested in a closed loop. The effects of fin configuration, including fin size, fin pitch, on the heat transfer rate and air-side pressure drop were analyzed. Moreover, new correlations of heat transfer for fin-and-tube heat exchanger with 5 mm diameter tubes were developed, and correlations agree with the experiment data well.

2. FIN CONFIGURATION DESIGN

Fin configuration suitable for 5 mm diameter fin-and-tube heat exchanger is designed by the method shown in Fig. 1. The fin size and fin pattern which mainly affect heat transfer and air pressure drop are designed by a Computational Fluid Dynamic (CFD) – based method.

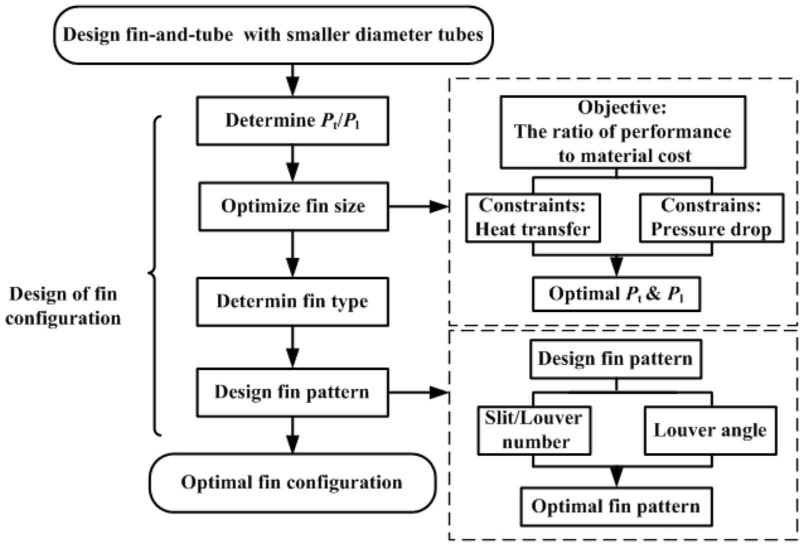

Figure 1. The scheme of design method of heat exchanger with microgroove smaller tubes

2.1 Determine the optimal ratio of P_t to P_l

In this study, the optimal ratio of P_t to P_l refers to that of fin with the highest fin efficiency among fins which have the same area. The fin efficiency is defined as the ratio of the actual fin heat transfer capacity ($Q_{\mathrm{actual,fin}}$) to the maximum possible heat transfer capacity ($Q_{\mathrm{ideal,fin}}$) if the entire fin were at the base temperature, as Eq. (1) shown:

$$\eta = \frac{Q_{\mathrm{actual,fin}}}{Q_{\mathrm{ideal,fin}}}, \qquad (1)$$

Both of $Q_{\mathrm{actual,fin}}$ and $Q_{\mathrm{ideal,fin}}$ are calculated by CFD method. In CFD calculation, the values of P_t/P_l are selected in the range of commonly used P_t/P_l of heat exchangers in air conditioners. The geometrical models are selected as the fin-and-tube with 2-rows tubes. The boundary conditions are: 1） Air inlet temperature is set as 300 K；2）The tube wall temperature is set as 280 K.；3）The fin is coupled with tube wall in the model of actual fin, and the fin temperature is set as the same with that of tube wall in the model of ideal fin； 4）The upper and under air surface are defined as periodic surface without pressure drop. From the CFD result in Fig. 2, the best P_t/P_l can be easily determined as 1.23 where the fin efficiency reaches the highest value.

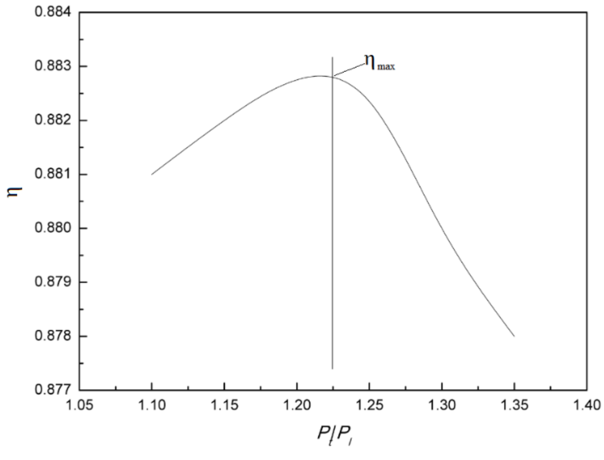

Figure 2. Variations of fin efficiency as function of wind velocity

2.2 Optimize fin size

For evaporator, the louver or slit will be blocked by condensate film which forms in refrigeration conditions, so the louver or slit fin is like a plate fin. Thus, this method employs the correlations for plate fin to determine fin size.

In fin size optimization, one objective function is used to analyze the ratio of performance to material cost as Eq. (2) shown. And two constraint functions, in Eq. (3) and (4), are that the *UA* of fin for smaller tubes should be equal to or larger than requirement, and the air pressure drop should be equal to or lower than requirement.

$$\max w = \frac{UA}{C}, \tag{2}$$

$$UA > UA_{require}, \tag{3}$$

$$\Delta P < \Delta P_{require}, \tag{4}$$

For 5 mm diameter fin-and-tube heat exchanger, The *UA* should be higher than that of plate fin for 7 mm diameter tubes, and the ΔP should be smaller than that of plate fin for 7 mm diameter tubes. Based on the above design principle, the variations of heat transfer coefficient, air pressure drop and the ratio of performance to material cost as function of the P_t are calculated and shown in Fig. 3 (a) to (c). From the results, the best P_t can be determined as 18 mm which has high *w* and also satisfies the constraints of *UA* and ΔP. From the optimal P_t/P_l, the optimal fin size is determined as 18×14.7 mm.

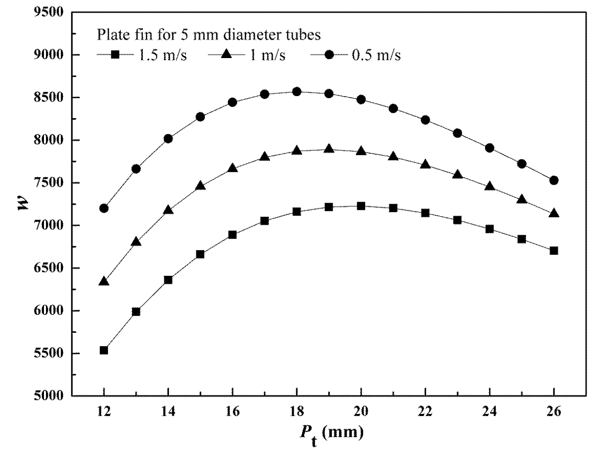

(a)

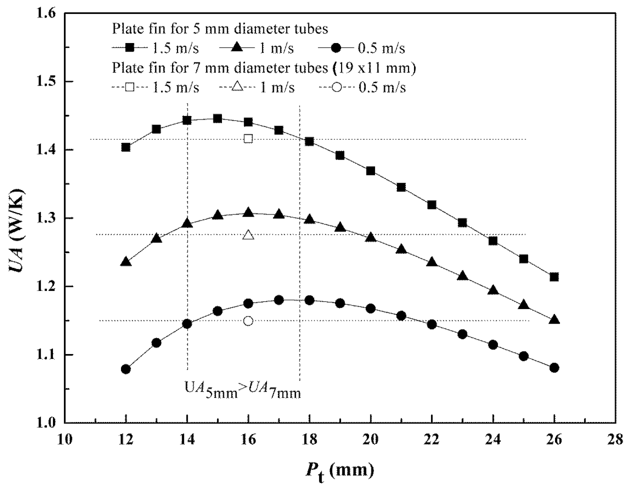

(b)

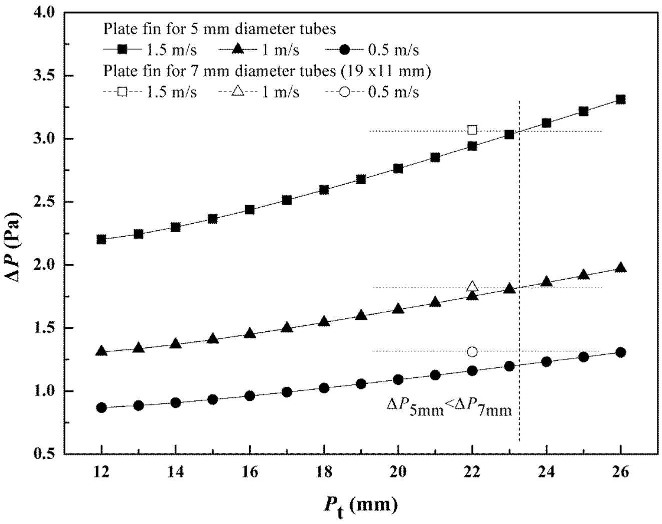

(c)

Figure 3. Variations of *w*, *UA* and Δ*P* as function of P_t: (a. Ratio of performance to material cost-*w*; b. Heat transfer performance-*UA*; c. Air pressure drop-Δ*P*)

2.3 Optimize fin pattern

In fin pattern optimization, because of no empirical correlation for predicting the performance of enhanced fin-and-tube with smaller diameter tubes is published, the CFD method is used to simulate the heat transfer capacity and air pressure drop of heat exchangers in this study.

Louver fin can break air boundary more easily than slit fin. In this study, louver fin is chosen to be designed. For louver fin, the louver angle and louver number are independent variables, while louver height and louver pitch are determined by two independent variables. With the limitation of manufacture, the louver is usually 25˚. Thus, the only independent variable is louver number.

Based on the optimal fin size, the performances of fins with 3 louvers and 4 louvers are calculated by CFD method. Fig. 4 shows the temperature distributions on fin surface. Table 1 shows the results of heat transfer capacity and air pressure drop of heat exchanger. From results, the fin with 4 louvers has higher heat transfer capacity, and smaller air pressure drop than those of fin with 3 louvers which are caused by the more louver number but lower louver height. Thus, the optimal fin pattern is the louver fin with 4 louvers.

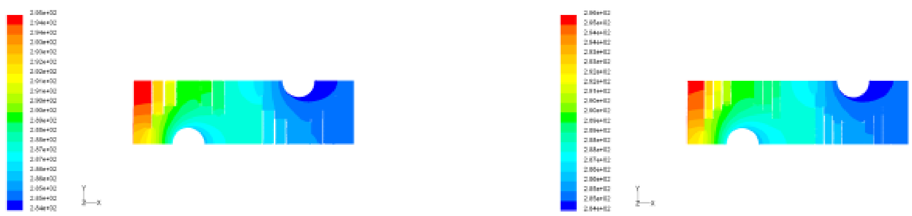

(a) Louver fin with 3 louvers (b) Louver fin with 4 louvers

Figure 4. CFD results of temperature distribution on louver fins with different patterns

Table 1: Heat transfer capacity and air pressure drop of louver fins with different pattern

Louver angle	Louver number	Heat transfer capacity (W)	Air pressure drop (Pa)
25^o	3	16.35	17.10
	4	16.53	16.75

3. EXPERIMENT

Based on the design results, a set of fin for fin-and-tube heat exchanger with 5 mm diameter tubes is tested to develop correlations to predict the performance of fin-and-tube heat exchanger with 5 mm diameter tubes. The test samples are 11 fin-and-tube heat exchangers which consist of aluminum fins and copper tubes with different fin sizes, fin pitches and rows, but with the same louver number because of manufacture limitation. The detailed fin configurations are shown in Table 2.

Table 2: Geometric dimension of the tested fin-and-tube heat exchangers

$P_t \times P_l$ (mm×mm)	δ (mm)	D_c (mm)	F_p (mm)	Row number	Fin pattern and details
19×11	0.095	5.2	1.2/1.4	1	3 louvers
19×13.6	0.095	5.2	1.1/1.2/1.4	1	3 louvers
18×13.8	0.095	5.2	1.2/1.3/1.4	1	3 louvers
18×14.7	0.095	5.2	1.2/1.3/1.4	2	3 louvers

3.1 Experimental apparatus

The experimental apparatus including an air flow loop, a water flow loop, a data acquisition system and the test heat exchangers are shown in Fig. 5.

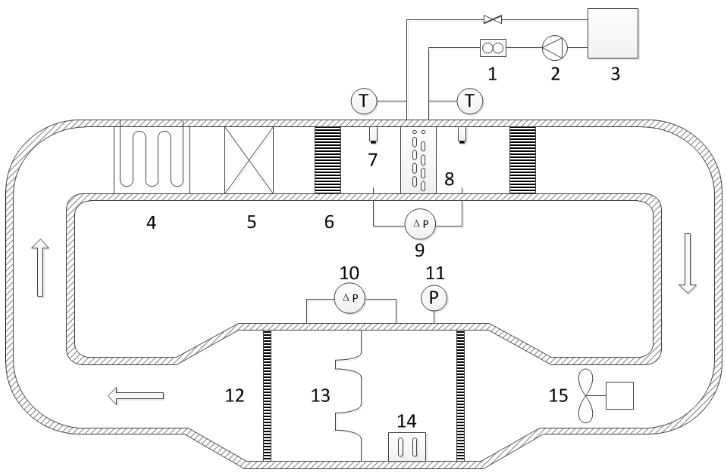

Figure 5. Schematic of experimental system

The air flow loop is a close type wind tunnel. A variable speed centrifugal fan (0.75 kW) is used to circulate the air passing through the nozzle chamber, the air conditioner box, the mixing device, the straightener, and the test heat exchanger orderly. A pressure transmitter (GE Druck, model PTX 1400) with ±1.0 kPa precision and a dry bulb and wet bulb temperature transducer (CHINO, model R220-30) with ±0.3K precision are used to measure the inlet air conditions of nozzles. Air pressure difference across nozzle is measured by a differential pressure transmitter (GE Druck, model LPM 9000) with ±5.0 Pa precision. Multiple nozzles based on the ASHRAE 41.2 standard (1987) are used to measure the air flow rate. The air conditioner box is used to control the temperature and humidity of air at test section inlet, which are allowed ±0.2 K and ±3% fluctuation range. A 20 mm thick thermal insulation material is used to insulate the test section to avoid heat transference between the heat exchanger and air. The dry bulb temperature and relative humidity of air at inlet and outlet of test section are measured by two temperature and humidity transducers (VAISALA, model HMP 233) with ±0.1 K and ±1.4% precision. Six K-type thermocouples with ±0.1 K precision welded on the tube surface are used to measure the fin base temperature. A differential pressure transmitter (GE Druck, model LPM 9481) with ±0.2 Pa precision is used to measure the pressure difference across the heat exchangers.

The water flow loop consists of a thermostat (ADVANTEC, model TBH 127AA), a centrifugal pump and a magnetic flow meter (TOKYO KEISO, model MGM 1010K) with ±0.15 L/min precision. Cold water is used as heat transfer fluid on the tube side. Water loop is aimed to provide the cool capacity of the test heat exchangers. Water is pumped out of the thermostat, delivered to the heat exchanger and then returned to the thermostat, when it reaches the required temperature. The water temperature differences between inlet and outlet of heat exchangers are measured by two K-type thermocouples with a calibrated accuracy of ±0.1 K. All signals are registered by a data acquisition system and finally averaged over the elapsed time. Total 14 test conditions are listed in Table 3.

Table 3. The test conditions

RH_{in} (%)	$T_{a,in}$ (K)	$T_{w,in}$ (K)	V (m/s)
40	300	283	0.5/1.0/1.5
50	300	283	0.5/0.8/1.0/1.2/1.5
65	300	283	0.5/1.0/1.5
80	300	283	0.5/1.0/1.5

3.2 Data reduction

The reduction process is based on the Threlkeld (1970) method which is an enthalpy-based reduction method. Some important reduction procedures are described as follows. More details can be found in previous study (Wu et al., 2012). In the experiments, only those data that satisfy the ASHRAE 33-78 (2000) requirements (the energy balance conditions, $|Q_w - Q_a|/Q_{ave} \leq 0.05$) are considered in the final analysis.

The total heat transfer coefficient of heat exchanger can also be calculated as Eq. (8), where the fin efficiency is defined under partially wet condition:

$$\frac{1}{U_{o,w}} = \frac{b_r' A_o}{h_i A_{p,i}} + \frac{b_p' A_o \ln\left(\frac{D_c}{D_i}\right)}{2\pi k_p L_p} + \frac{b_{w,p}' A_o}{h_{o,w}\left(A_{p,o} + \eta_{f,wet} A_f\right)}, \tag{8}$$

Heat transfer coefficient in tube can be calculated as:

$$h_i = \left(\frac{k_i}{D_i}\right)\frac{\left(\mathrm{Re}_{Di} - 1000\right)\mathrm{Pr}\left(f_i/2\right)}{1 + 12.7\sqrt{f_i/2}\left(\mathrm{Pr}^{2/3} - 1\right)}, \tag{9}$$

where,

$$f_i = \left[1.58\ln\left(\mathrm{Re}_{Di}\right) - 3.28\right]^{-2}, \tag{10}$$

j factor is presented as:

$$j = \frac{h_s}{G_c c_{p,a}}\mathrm{Pr}^{2/3}, \tag{11}$$

3.3 Results and discussion

Fig. 6 depicts the effect of fin pitch on air-side heat transfer performance of heat exchanger with 5 mm diameter tubes. The Colburn *j* factors decrease with the increases of fin pitch. Moreover, water bridge occurs at the bottom of fin with hydrophilic coating as Fig. 7 shows, which did not occur in fin-and-tube heat exchanger with 7 mm or 10.33 mm diameter tubes in previous studies (Ma et al., 2007 and 2009). The occurrence of water bridge may be due to the smaller fin size and fin pitch. When fin size decreases, the maximum coverage area of film decreases accordingly which leads to the height of condensate film increases. Then, the smaller fin pitch allows higher condensate films at adjacent fin surface to combine to a water bridge. However, because of the small coverage area and the bottom location of water bridge, the effects of relative humidity and fin pitch on heat transfer performance are similar to previous research (Ma et al., 2007 and 2009) in which no water bridge occurred on the fin surface.

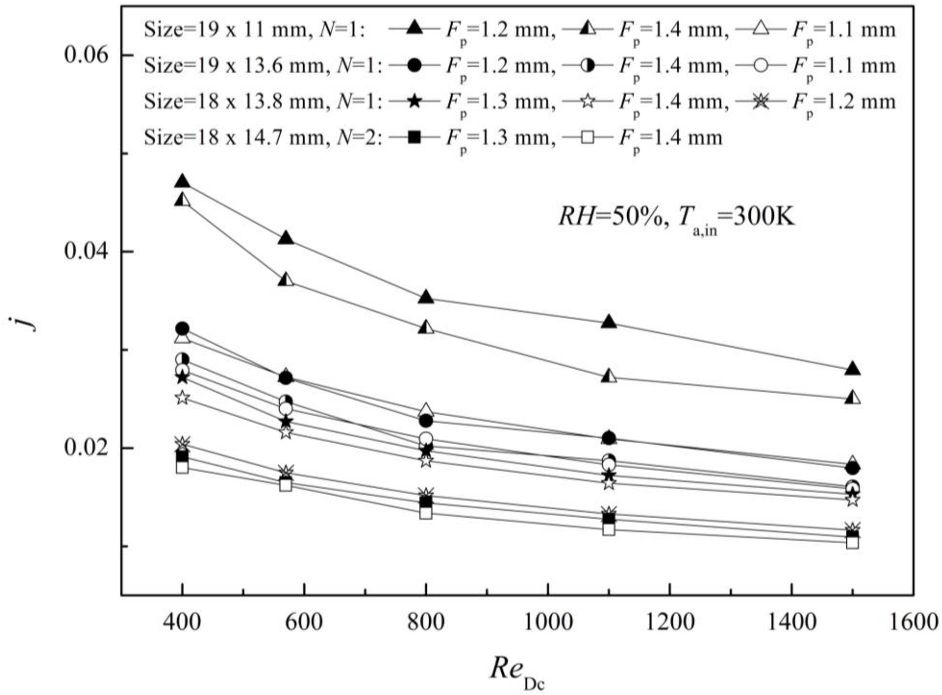

Figure 6: Variations of Colburn *j* factor as function of air Reynolds number

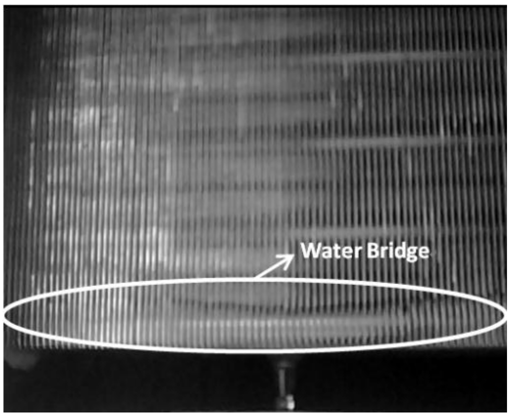

Figure 7: The location of water bridge on fin for 5 mm diameter tubes

4. CORRELATIONS

The multiple linear regression technique in a practical range of experimental data (350 < Re_{Dc} < 4500) is carried out, and the suitable correlation of *j* is given as follows:

$$j = 0.0899\,\mathrm{Re}_{Dc}^{-0.4228}\left(\frac{P_t}{P_l}\right)^{1.9513}\left(\frac{F_p}{D_c}\right)^{-0.5677} N^{-0.2712}, \quad (12)$$

Range for applicability for Eq. (12) is given as follows: D_c=5.2 mm, P_t=18-19 mm, P_l=11-14.7 mm, F_p=1.1-1.4 mm, *N*=1-2, Re_{Dc}=350-4500.

The proposed heat transfer *j* factor correlation, Eq. (12), can describe 85.7% of the test data within the deviation of ±15%. The proposed correlation of *j* has a mean deviation of 6.5%.

5. CONCLUSIONS

(1) Optimal louver fin configuration for 5 mm fin-and-tube heat exchanger is designed by Computational

Fluid Dynamic method.

(2) Water bridge occurs at the bottom of fin with hydrophilic coating, which did not occur in fin-and-tube heat exchangers with 7 mm or 10.33 mm diameter tubes in previous studies.

(3) Correlation of *j* is developed to predict the heat transfer rate of fin-and-tube heat exchanger with 5 mm diameter tubes. The mean deviation of the proposed *j* correlation is 6.5%.

NOMENCLATURE

A	heat transfer area (m^2)	C	material cost (kg)
D	diameter (m)	F	fiction factor fb
F_p	fin pitch (m)	G_c	mass flus ($kgm^{-2}s^{-1}$)
h	convection heat transfer coefficient ($Wm^{-2}K^{-1}$)	i	enthalpy ($kJkg^{-1}$)
I_0	Bessel function solution of the second kind, order 0		
I_1	Bessel function solution of the second kind, order 1		
j	Colburn heat transfer factor		
K_0	Bessel function solution of the first kind, order 0		
K_1	Bessel function solution of the first kind, order 1		
N	Row number of tubes	P_t	transverse tube pitch (m)
P_l	longitudinal tube pitch (m)	ΔP	pressure drop (Pa)
Q	heat transfer capacity (W)	Re_{Dc}	Reynolds number based on the outer tube diameter
δ	fin thickness (m)		

Subscripts

a	air	f	fin
fb	fin base	ft	fin tip
i	inner	in	inlet
o	outer	r	refrigerant
s	saturate	w	water

REFERENCES

Threlkeld T., 1970, Thermal Environment Engineering, Prentice-Hall, New York, p. 257–259.

Ma, X.K, Ding, G.L., Zhang, Y.M., et al., 2007, Airside heat transfer and friction characteristics for enhanced fin-and-tube heat exchanger with hydrophilic coating under wet conditions, Int. J. Refrig., vol. 30: p. 1135-1167.

Ma, X.K, Ding, G.L., Zhang, Y.M., et al., 2009, Airside characteristics of heat, mass transfer and pressure drop for heat exchangers of tube-in hydrophilic coating wavy fin under dehumidifying conditions, Int. J. Heat and Mass Transfer, vol. 52, no. 19-20: p. 4358-4370.

Wang, C.C., Lee, W.S., Sheu, W.J., et al, 2002, A comparison of the airside performance of the fin-and-tube heat exchangers in wet conditions with and without hydrophilic coating, Appl. Thermal Eng, vol. 22: p. 269–278.

Wu, W., Ding, G.L., Gao, Y.F., et al, 2012, Experimental investigation of fin-and-tube heat exchanger with smaller diameter tubes. The 6th Asian Conference on Refrigeration and Air Conditioning, August 26-28, 2012, Xi'an, China.